Journal of
Materials Chemistry A

PAPER

View Article Online
View Journal | View Issue

General acid and base bifunctional graphene oxide for cooperative catalysis†

Cite this: *J. Mater. Chem. A*, 2014, **2**, 10239

Wenfeng Zhang, Hanying Gu, Zhen Li, Yuanzhi Zhu, Yang Li, Guoliang Zhang, Fengbao Zhang and Xiaobin Fan*

Received 26th March 2014
Accepted 29th April 2014

DOI: 10.1039/c4ta01446d

www.rsc.org/MaterialsA

In this study, a bifunctional graphene oxide material (GO–AEP–UDP) with a general acid, the ureidopropyl (UDP) group, and a general base, the 3-[2-(2-aminoethylamino)ethylamino]-propyl (AEP) group, was synthesized by silylanization of graphene oxide (GO) with organoalkoxysilane precursors. Characterization of the obtained GO–AEP–UDP was carried out by Fourier transform infrared spectroscopy (FTIR), Raman spectroscopy, scanning electron microscopy (SEM), energy dispersive spectroscopy (EDS), high-resolution transmission electron microscopy (HRTEM), X-ray photoelectron spectroscopy (XPS) and zeta potential measurements. Systematic studies demonstrated that GO–AEP–UDP has superior catalytic performance in the classic Henry reaction of 4-nitrobenzaldehyde with nitromethane. It was found that the relative concentration and spatial arrangement of cooperative functional groups were very important factors in the synergistic catalysis.

1. Introduction

Organocatalysis is a powerful methodology in organic synthesis, and organocatalysts have remarkable advantages over traditional transition-metal catalysts such as insensitivity to moisture and oxygen, ready availability and low toxicity.[1–9] However, the application of organocatalysts in the chemical industry is still limited, attributed to not only their relatively low catalytic activities (especially compared with many metal complexes), but also the difficulty in separation from the reaction mixtures. Therefore, development of a recyclable organocatalyst with high catalytic performance is of great importance due to its practical application on an industrial scale. Among the strategies that have been developed for recycling the organocatalysts, the preparation of heterogeneous organocatalysts is the most promising one. So far, lots of organic acid/base catalysts and their bifunctional systems have been successfully immobilized on various solid supports and have shown impressive catalytic performances in a variety of reactions.[10–30] Recently, we and others found that graphene supported phenyl–SO_3H groups, amine groups and phosphotungstic acid show excellent catalytic activities and robustness in the hydrolysis rate of ethyl acetate, nitroaldol reaction and one-pot tandem reaction.[31–33] However, to the best of our knowledge, the cooperation of general acid and base groups immobilized on graphene has yet to be demonstrated in chemical reactions.

Herein, we report the first graphene supported general acid and base bifunctional catalytic system that comprises a general acid, the ureidopropyl (UDP) group, and a general base, the 3-[2-(2-aminoethylamino) ethylamino]propyl (AEP) group. We also found that this catalytic system has an excellent catalytic performance in the cooperative Henry reaction of 4-nitrobenzaldehyde with nitromethane.

2. Experimental

2.1. Preparation of the general acid/base–graphene oxide catalyst

Graphene oxide (GO) was prepared and purified by the Hummers method.[34] The resulting GO suspension (15 mL, 19.4 mg mL^{-1}) was sonicated for 30 min. It was then added to the mixture of ethanol (150 mL), ureidopropyltrimethoxysilane (0.8877 g), and 3-[2-(2-aminoethylamino)ethylamino]propyltrimethoxysilane (0.2228 g) in a three-necked round flask with a condenser and a stirrer. After 24 h refluxing at 78 °C, the black solid was filtered and washed with ethanol and deionized water successively, followed by drying under vacuum to get GO–AEP–UDP.

2.2. Catalytic ability

The performance of the catalysts was examined by the Henry reaction. Into a round flask were placed the catalyst (10 mg), 4-nitrobenzaldehyde (1 mmol) and nitromethane (10 mL). The resulting mixture was vigorously stirred for 24 h at 90 °C. After

---

State Key Laboratory of Chemical Engineering, School of Chemical Engineering & Technology, Tianjin University, Tianjin, China. E-mail: xiaobinfan@tju.edu.cn; Fax: +86-22-27408778; Tel: +86-22-27408778

† Electronic supplementary information (ESI) available: Si 2p XPS spectrum and HRTEM spectrum of GO–AEP–UDP, photographs and GC-MS results of the product, and mechanism of the catalytic reaction. See DOI: 10.1039/c4ta01446d

the catalyst was separated from the mixture by filtration, the filtrate was analyzed by GC.

2.3. Characterization

The samples were characterized by Fourier transform infrared spectroscopy (FTIR) (Thermo-Nicolet 380), Raman spectroscopy (NT-MDT NTEGRA Spectra), scanning electron microscopy (SEM) (Hitachi S4800), energy dispersive spectroscopy (EDS) (Hitachi S4800), high-resolution transmission electron microscopy (HRTEM) (Philips Tecnai G2 F20), zeta potential measurements (Malvern, nano ZS) and X-ray photoelectron spectroscopy (XPS) (PerkinElmer, PHI 1600 spectrometer). The reactions were monitored using a GC (Agilent 6890N GC-FID system) and GC-MS (Agilent 6890-5973).

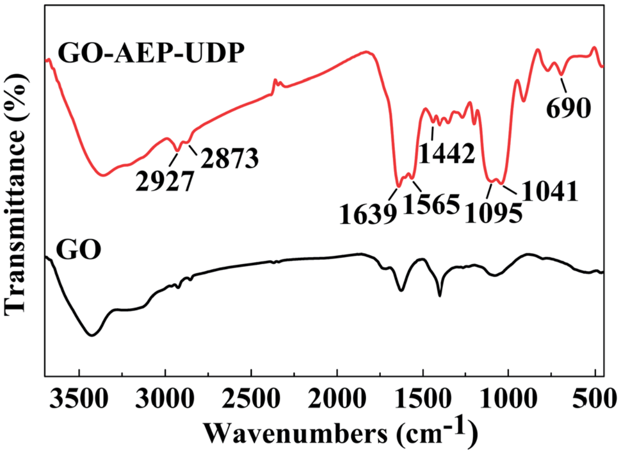

Fig. 1 FTIR spectra of GO and GO–AEP–UDP.

3. Results and discussion

The bifunctional graphene oxide material with ureidopropyl (UDP) and 3-[2-(2-aminoethylamino)ethylamino]propyl (AEP) groups was synthesized by introducing UDP–, AEP–trimethoxysilane precursors to the silylanization reaction that is based on the hydrolysis and dehydration condensation of the silanes with the hydroxyl and epoxy groups on GO (Scheme 1).

The catalysts were characterized after the functionalization. Fig. 1 shows Fourier transform infrared spectroscopy (FTIR) spectra of the samples of GO and GO–AEP–UDP. Compared with GO, the peaks at 1639 cm^{-1} and 1565 cm^{-1} are associated with C$=$O stretching vibrations of the UDP group and N–H bending vibrations of the AEP group, respectively. The increased doublets at 2927 cm^{-1} and 2873 cm^{-1}, together with a new band at 1442 cm^{-1}, represent the stretching and bending vibrations of C–H from the methyl groups of UDP and AEP groups. The signal of O–H becomes smaller after formation of GO–AEP–UDP. In addition, the strong stretching vibrations of Si–O at 1041 cm^{-1}, as well as the obvious stretching and bending vibrations of Si–O–C at 1095 and 690 cm^{-1}, demonstrate that the silylanization reaction proceeded successfully.

Raman spectroscopy was used to characterize the structural change of graphene oxide in the chemical process, as can be seen in Fig. 2. GO shows absorption at 1584 cm^{-1} corresponding to the G-band. While the G-band of GO–AEP–UDP shifts to 1594 cm^{-1} after the silylation reaction, implying the increased compressive local stress induced by the attached AEP and UDP groups. Moreover, the *I*(D)/*I*(G) intensity ratio of GO–AEP–UDP (1.895) is slightly higher than that of GO (1.478); this means that abundant AEP and UDP groups were introduced to the sp^2 carbon network; this conclusion was further supported by our XPS analysis.

The X-ray photoelectron spectroscopy (XPS) spectra of the samples of GO and GO–AEP–UDP are shown in Fig. 3. In comparison to GO, the increased signals of C, O, N, and Si were observed in GO–AEP–UDP (Fig. 3a). Furthermore, a significant decrease of the C–O–C & C–OH bonds and a slight increase of the carboxyl groups in the C 1s peak (Fig. 3c and d), together with the formation of Si–O–C observed at 102.4 eV in the Si 2p XPS spectrum (Fig. S1 of ESI†), indicate the successful hydrolysis and dehydration condensation of the hydroxyl and epoxy groups on GO with the AEP– and UDP–trimethoxysilane precursors. Moreover, the peak at 399.1 eV corresponds to C–NH–C of AEP groups, another one at 399.8 eV represents

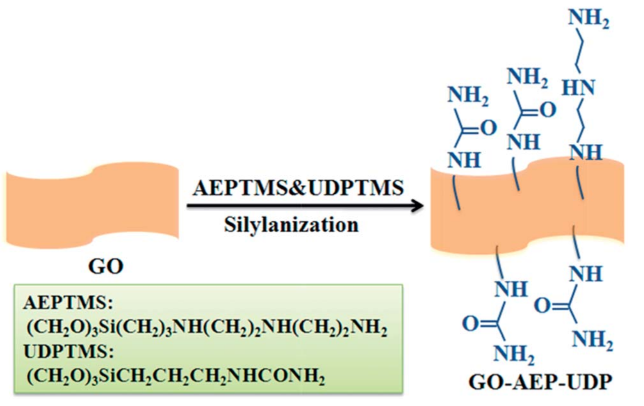

Scheme 1 Illustration of the preparation of the general acid/base bifunctional catalyst.

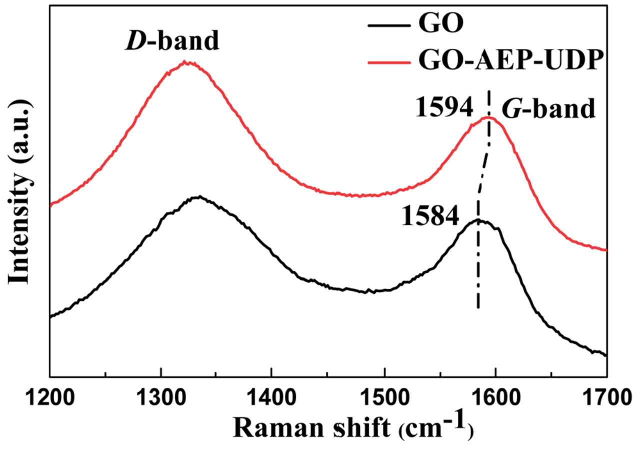

Fig. 2 Raman spectra of GO and GO–AEP–UDP.

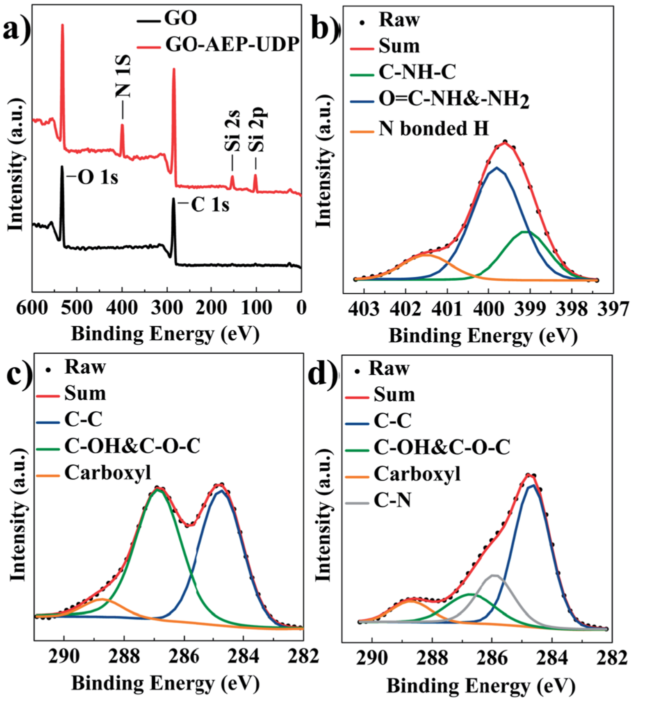

Fig. 3 XPS spectra of GO and GO–AEP–UDP (a), N 1s XPS spectra of GO–AEP–UDP (b), C 1s XPS spectra of (c) GO and (d) GO–AEP–UDP.

$-NH_2$ and O=C–NH of UDP groups in the N 1s spectrum (Fig. 3b). Calculated by the two integral areas, the molecule ratio of AEP and UDP groups is about 1 : 4. Note that the element atomic ratios of N in GO–AEP–UDP are 9.62%, That is, the density of the introduced AEP and UDP groups is about 0.62 and 2.48 mmol g^{-1}, respectively.

Fig. 4 shows the zeta potential of GO and GO–AEP–UDP. GO displays a zeta potential of −26.6 mV under neutral conditions because of the negatively charged carboxylate groups. However, GO–AEP–UDP shows positively charged surfaces with a zeta potential of 26.8 mV, which is assigned to the abundant grafted amine groups. The successful silylation reaction was verified again.

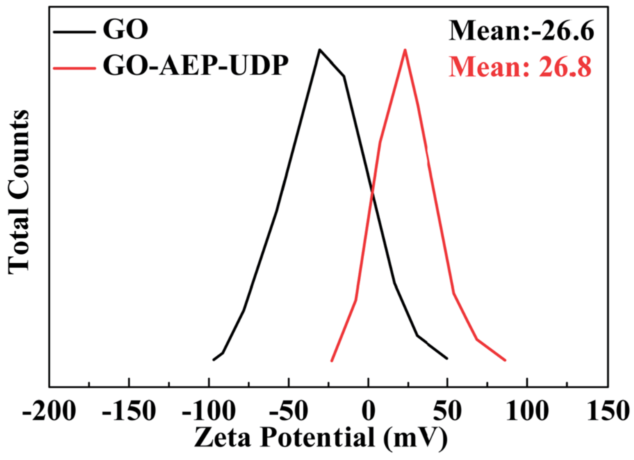

Fig. 4 The zeta potentials of GO and GO–AEP–UDP.

Fig. 5 shows the scanning electron microscopy (SEM) images and the corresponding quantitative energy dispersive X-ray spectroscopy (EDS) mapping of GO–AEP–UDP. Fig. 5a reveals that GO–AEP–UDP shows a crumpled structure that can also be observed in the HRTEM image (Fig. S2 of ESI†). Element distribution analysis demonstrates that elements O, Si, and N (Fig. 5b–d) are homogeneously distributed on the whole surface of GO–AEP–UDP, which indicates that AEP and UDP groups are anchored on GO uniformly. These features of GO–AEP–UDP make active sites utilize efficiently, because all the active sites located on the surface of the layer are accessible, which will render GO–AEP–UDP efficient for the catalytic reaction.

The catalytic efficiency of the resultant GO–AEP–UDP catalyst was investigated by using the Henry reaction of 4-nitrobenzaldehyde and nitromethane to *p*,β-dinitrostyrene (Scheme 2). The first step of this reaction is the classic nucleophilic addition of aldehyde and nitromethane to nitroalcohol,[35–37] followed by intramolecular dehydration of the –OH with the *ortho*-H of nitroalcohol at high temperature (GC-MS results of the final products can be seen in Fig. S3 of ESI†). Note that equivalent amounts of GO, GO–UDP and GO–AEP were also examined for comparison purposes, and the results are presented in Table 1.

Yields of the products catalyzed by GO, GO–UDP, GO–AEP and GO–AEP–UDP are 3.2%, 12.2%, 6.7% and 88.4%, respectively (entries 1, 2, 3, and 5 in Table 1), which is in accordance with the product color (Fig. S4 of ESI†); a synergistic effect between the AEP and UDP groups was clearly observed. This result can be explained by the fact that the secondary amines of the AEP group were responsible for the deprotonation of CH_3NO_2,[38] and the UDP group could activate the carbonyl group of 4-nitrobenzaldehyde to nucleophilic attack through double

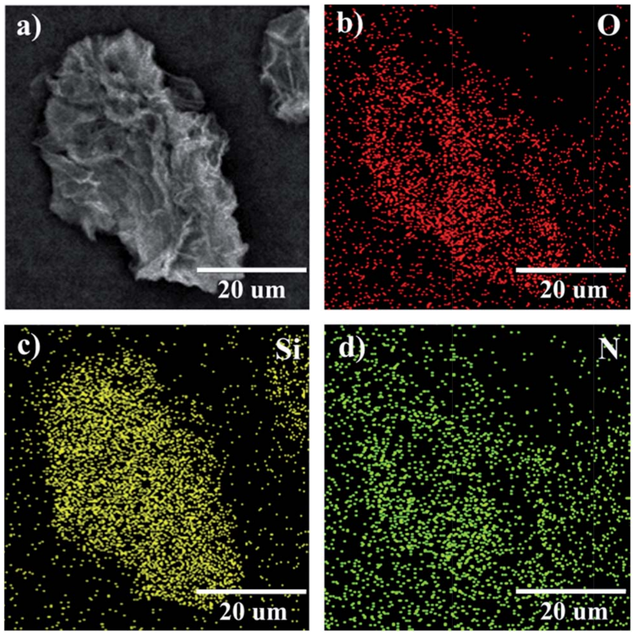

Fig. 5 SEM image of (a) GO–AEP–UDP and the corresponding quantitative EDS element mapping of (b) O, (c) Si and (d) N.

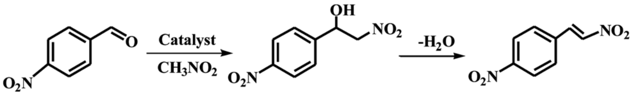

Scheme 2 The catalytic preparation of *p*,β-dinitrostyrene from 4-nitrobenzaldehyde and nitromethane.

Table 1 Performances of different catalysts in the Henry reaction[a]

Rank	Catalyst	Yield (%)	TON[b]
1	GO	3.2	—
2	GO–UDP	12.2	16.9
3	GO–AEP	6.7	9.0
4	Heterogeneous mixture[c]	1.8	2.5
5	GO–AEP–UDP[d]	88.4	124.5
6	Homogeneous mixture	11.5	6.78

[a] Reaction conditions: 4-nitrobenzaldehyde (1 mmol), CH_3NO_2 (10 mL), catalyst (10 mg), 90 °C, 24 h. [b] TON (turnover number) = mmol product per mmol catalyst for a 24 h reaction time with 10 mg of catalysts. [c] GO–AEP (2 mg) + GO–UDP (8 mg). [d] The initial molar ratio of AEP/UDP = 1/4.

hydrogen bonding[39] (the mechanism can be seen in Fig. S5 of ESI†). The yield of the product by using the heterogeneous mixture with GO–AEP and GO–UDP (1.8%, entry 4 in Table 1) was clearly lower than that by using GO–AEP–UDP (88.4%); this result suggests that spatial arrangements between these active molecules are crucial for this reaction. Note that the homogeneous mixture of AEP and UDP gives a poor yield of 11.5% (entry 6 in Table 1) due to a large amount of byproducts. The turnover numbers (TONs) of these catalysts give similar results; GO–AEP–UDP gives the best performance with a TON of 124.5. Compared with the existing studies on silica-based catalysts,[40–43] the TON of our catalyst GO–AEP–UDP is comparable to (if not better than) most of the existing catalysts. This promising result should be attributed to the two-dimensional GO that not only provides a large surface to support the catalytically active sites but also facilitates the mass transport process.

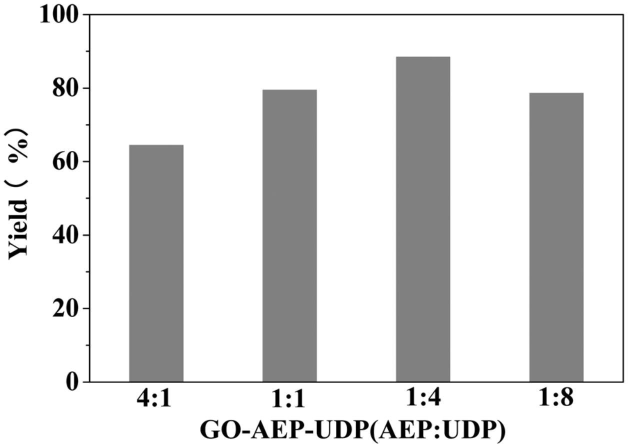

Fig. 6 Yields of the products catalyzed by the catalyst with different ratios of AEP and UDP groups.

To further evaluate the synergistic effect of GO–AEP–UDP, catalysts with different relative concentrations, initial molar ratios of the organoalkoxysilane precursors as AEP/UDP = 4/1, 1/1, 1/4 and 1/8, were synthesized and systematically studied for their catalytic performances. As summarized in Fig. 6, the catalyst with an AEP/UDP ratio of 1 : 4 shows the highest catalytic activity with a yield of 88.4% towards the product.

4. Conclusions

In conclusion, we have successfully prepared a bifunctional graphene oxide material that comprises a general acid group, UDP, and a general base group, AEP, by silylanization. Systematic studies demonstrated that these active groups could be readily loaded on both sides of graphene oxide sheets with homogeneous distribution. Notably, the obtained bifunctional graphene oxide materials (GO–AEP–UDP) show excellent catalytic performances and synergistic catalytic effect in the Henry reaction. By adjusting the relative concentrations and spatial arrangement of the cooperative functional groups, our bifunctionalized graphene-based catalyst could have better application prospects in other organic reactions.

Acknowledgements

This study was supported by the National Natural Science Funds for Excellent Young Scholars (no. 21222608), Program for New Century Excellent Talents in University (no. NCET-12-0392), Research Fund of the National Natural Science Foundation of China (no. 21106099), Foundation for the Author of National Excellent Doctoral Dissertation of China (no. 201251) and the Programme of Introducing Talents of Discipline to Universities (no. B06006).

References

1 M. Gaunt, *Nature*, 2011, **470**, 183–185.
2 B. List and J. W. Yang, *Science*, 2006, **313**, 1584–1586.
3 R. N. Butler and A. G. Coyne, *Chem. Rev.*, 2010, **110**, 6302–6337.
4 J. Mlynarski and S. Bas, *Chem. Soc. Rev.*, 2014, **43**, 577–587.
5 D. Enders, C. Grondal and M. R. M. Hüttl, *Angew. Chem., Int. Ed.*, 2007, **46**, 1570–1581.
6 K. Matsui, S. Takizawa and H. Sasai, *J. Am. Chem. Soc.*, 2005, **127**, 3680–3681.
7 L.-W. Xu, J. Luo and Y. Lu, *Chem. Commun.*, 2009, 1807–1821.
8 N. Marion, S. Díez-González and S. P. Nolan, *Angew. Chem., Int. Ed.*, 2007, **46**, 2988–3000.
9 P. Melchiorre, M. Marigo, A. Carlone and G. Bartoli, *Angew. Chem., Int. Ed.*, 2008, **47**, 6138–6171.
10 J.-W. Lee, T. Mayer-Gall, K. Opwis, C. E. Song, J. S. Gutmann and B. List, *Science*, 2013, **341**, 1225–1229.
11 P. MacLellan, *Nat. Chem.*, 2013, **5**, 896–897.
12 Y. Wei and M. Shi, *Chem. Rev.*, 2013, **113**, 6659–6690.

13 M. Raynal, P. Ballester, A. Vidal-Ferran and P. W. N. M. van Leeuwen, *Chem. Soc. Rev.*, 2014, **43**, 1660–1733.

14 M. Gruttadauria, F. Giacalone and R. Noto, *Chem. Soc. Rev.*, 2008, **37**, 1666–1688.

15 V. N. Wakchaure and B. List, *Angew. Chem., Int. Ed.*, 2010, **49**, 4136–4139.

16 K. Motokura, M. Tada and Y. Iwasawa, *J. Am. Chem. Soc.*, 2009, **131**, 7944–7945.

17 J. D. Bass, A. Solovyov, A. J. Pascall and A. Katz, *J. Am. Chem. Soc.*, 2006, **128**, 3737–3747.

18 N. A. Brunelli, K. Venkatasubbaiah and C. W. Jones, *Chem. Mater.*, 2012, **24**, 2433–2442.

19 S. L. Jain, A. Modak and A. Bhaumik, *Green Chem.*, 2011, **13**, 586–590.

20 R. K. Zeidan and M. E. Davis, *J. Catal.*, 2007, **247**, 379–382.

21 M. J. Climent, A. Corma, H. Garcia, R. Guil-Lopez, S. Iborra and V. Fornés, *J. Catal.*, 2001, **197**, 385–393.

22 P. Li, C.-Y. Cao, Z. Chen, H. Liu, Y. Yu and W.-G. Song, *Chem. Commun.*, 2012, **48**, 10541–10543.

23 D. J. Coady, K. Fukushima, H. W. Horn, J. E. Rice and J. L. Hedrick, *Chem. Commun.*, 2011, **47**, 3105–3107.

24 K. Arnold, A. S. Batsanov, B. Davies, C. Grosjean, T. Schutz, A. Whiting and K. Zawatzky, *Chem. Commun.*, 2008, 3879–3881.

25 M. J. Climent, A. Corma, V. Fornés, R. Guil-Lopez and S. Iborra, *Adv. Synth. Catal.*, 2002, **344**, 1090–1096.

26 T. Miura, K. Imai, M. Ina, N. Tada, N. Imai and A. Itoh, *Org. Lett.*, 2010, **12**, 1620–1623.

27 X. Li, Y. Yang and Q. Yang, *J. Mater. Chem. A*, 2013, **1**, 1525–1535.

28 A. R. Moosavi-Zare, M. A. Zolfigol, V. Khakyzadeh, C. Bottcher, M. H. Beyzavi, A. Zare, A. Hasaninejad and R. Luque, *J. Mater. Chem. A*, 2014, **2**, 770–777.

29 A. Zamboulis, N. Moitra, J. J. E. Moreau, X. Cattoen and M. Wong Chi Man, *J. Mater. Chem.*, 2010, **20**, 9322–9338.

30 S. El Hankari, B. Motos-Perez, P. Hesemann, A. Bouhaouss and J. J. E. Moreau, *J. Mater. Chem.*, 2011, **21**, 6948–6955.

31 J. Ji, G. Zhang, H. Chen, S. Wang, G. Zhang, F. Zhang and X. Fan, *Chem. Sci.*, 2011, **2**, 484–487.

32 W. Zhang, S. Wang, J. Ji, Y. Li, G. Zhang, F. Zhang and X. Fan, *Nanoscale*, 2013, **5**, 6030–6033.

33 W. Zhang, Q. Zhao, T. Liu, Y. Gao, Y. Li, G. Zhang, F. Zhang and X. Fan, *Ind. Eng. Chem. Res.*, 2013, **53**, 1437–1441.

34 A. Lerf, H. He, M. Forster and J. Klinowski, *J. Phys. Chem. B*, 1998, **102**, 4477–4482.

35 A. Ebru Aydin and S. Yuksekdanaci, *Tetrahedron: Asymmetry*, 2013, **24**, 14–22.

36 E. C. Constable, G. Zhang, C. E. Housecroft, M. Neuburger, S. Schaffner, W.-D. Woggon and J. A. Zampese, *New J. Chem.*, 2009, **33**, 2166–2173.

37 A. Chougnet and W.-D. Woggon, *Org. Synth.*, 2013, **90**, 52–61.

38 F. Gelman, J. Blum and D. Avnir, *Angew. Chem., Int. Ed.*, 2001, **40**, 3647–3649.

39 P. M. Pihko, *Angew. Chem., Int. Ed.*, 2004, **43**, 2062–2064.

40 S. Huh, H.-T. Chen, J. W. Wiench, M. Pruski and V. S. Y. Lin, *Angew. Chem., Int. Ed.*, 2005, **44**, 1826–1830.

41 Y. Long, M. Xie, J. Niu, P. Wang and J. Ma, *Appl. Surf. Sci.*, 2013, **277**, 288–292.

42 Y. Huang, S. Xu and V. S. Y. Lin, *Angew. Chem., Int. Ed.*, 2011, **50**, 661–664.

43 S. Shylesh, A. Wagner, A. Seifert, S. Ernst and W. R. Thiel, *Chem. –Eur. J.*, 2009, **15**, 7052–7062.